The role of deposition process on pressure dip formation underneath a granular pile

Mechanics of Materials 66 (2013) 160–171

Contents lists available at ScienceDirect

Mechanics of Materials

journal homepage: www.elsevier.com/locate/mechmat

The role of deposition process on pressure dip formation underneath a granular pile ☆

Jun Ai [a,b], Jin Y. Ooi [b,*], Jian-Fei Chen [c], J. Michael Rotter [b], Zhijun Zhong [b]

[a] Nottingham Centre for Geomechanics, The University of Nottingham, University Park, Nottingham NG7 2RD, UK
[b] Institute for Infrastructure and Environment, Joint Research Institute for Civil and Environmental Engineering, School of Engineering, The University of Edinburgh, Edinburgh, EH9 3JL Scotland, UK
[c] School of Planning, Architecture and Civil Engineering, Queen's University Belfast, Belfast, BT7 1NN North Ireland, UK

ARTICLE INFO

Article history:
Received 12 May 2013
Available online 14 August 2013

Keywords:
Granular pile
Base pressure
Pressure dip
Construction history
Arching effect
Granular flow

ABSTRACT

This paper describes an experimental investigation on the pressure dip phenomenon in a conical pile of granular solids. The roles of different deposition processes such as the pouring rate, pouring height and deposition jet size on the pressure dip formation were studied. Test results confirmed that the pressure dip is a robust phenomenon in a pile formed by top deposition. When the deposition jet radius is significantly smaller than the final pile radius (i.e. concentrated deposition), a dip developed in the centre as shown in previous studies. However, when the deposition jet radius is comparable to the final pile radius (i.e. diffuse deposition), the location of the dip moves towards the edge of deposition jet, with a local maximum pressure developed in the centre. For concentrated deposition, an increase in the pouring rate may enhance the depth of the dip and reduce its width, while an increase in the pouring height has only a negligible effect in the studied range. The results suggest the pressure dip is closely related to the initial location, intensity and form of downslope flows.

1. Introduction

Granular materials are in abundance in nature and are also estimated to constitute over 75% of all raw material feedstock to industry (Nedderman, 1992). They have been extensively studied by both the scientific and engineering-communities, and yet they sometimes display behaviour that is counter-intuitive and a full understanding remains elusive. One classic granular mechanics problem is that of a humble 'sandpile' in which a significant dip in the vertical pressure on the base is observed underneath the apex, at the location where a simple interpretation might expect the maximum pressure. This 'pressure dip' phenomenon is also relevant to the bulk handling of industrial solids because many different bulk solids are commonly stored in open stockpiles, particularly in the mining industry (Fig. 1). The design of a gravity reclaim system for a stockpile requires knowledge of the base pressure distribution underneath the stockpile. The same phenomenon may also occur in silos that are filled from a 'point source' which might be expected to result in an increase in the silo wall pressure near the highest wall contact, but thisphenomenon is not recognised at all in the silos literature.

The sandpile problem has been the subject of many analytical, numerical and experimental studies and some good reviews of the problem are available (e.g. Atman et al., 2005; Cates et al., 1998; Didwania et al., 2000; Savage, 1997, 1998). However, there is little consensus on the fundamental physics or the mechanics assumptions made in the many mathematical models of this apparently simple system, and quite contradictory results are often claimed. Several factors have been suggested to explain the pressure dip observed under the apex of a pile. These

* Corresponding author. Tel.: +44 131 650 5725; fax: +44 131 650 6781.
E-mail address: j.ooi@ed.ac.uk (J.Y. Ooi).

0167-6636/$ - see front matter © 2013 The Authors. Published by Elsevier Ltd. All rights reserved.
http://dx.doi.org/10.1016/j.mechmat.2013.08.005

Fig. 1. A typical industrial stockpile formed by top deposition from a conveyor.

include the presence of a base deflection (e.g. Lee and Herington, 1971; Savage, 1998; Trollope, 1956; Wiesner, 2000), pile construction history (Geng etal., 2001; Vanel et al., 1999), formation of a granular skeleton (Savage, 1997), particle size segregation (Liffman et al., 1992, 1994; Liffman et al., 2001), particle shape (Zuriguel and Mullin, 2008; Zuriguel et al., 2007), "Fixed Principal Axes (FPA)" of stress propagation (Wittmer et al., 1997; Wittmer et al., 1996), reduced density in the central zone of the pile due to deposition impact (Smid and Novosad, 1981) and increased shear mobilisation on the base due to the deposition process (Ai et al., 2013; Ai et al., 2011; Michalowski and Park, 2004). However, neither the relative importance nor theinterplay between these factors is at all clear and a comprehensive understanding of this phenomenon remains elusive. This study involved carefully designed experiments to investigate the base pressure profile under a conical pile of mini iron ore pellets.

A variety of measurement techniques have been used to measure the pressure distribution on the base of a granular pile, including pressure cells (Evesque et al., 1999; Hummel and Finnan, 1921; Jotaki and Moriyama, 1979; Lee and Herington, 1971; McBride, 2006; Ooi et al., 2008; Smid and Novosad, 1981; Trollope, 1956), registering the load on articulated base strips instrumented with strain gauges (Lee and Herington, 1971), strain gauges fixed on the base plate (Trollope, 1956), an elasto-optical method(Brockbank et al., 1997), single capacitive normal stress sensor (Vanel et al., 1999), and photoelastic methods (Geng et al., 2001; Zuriguel and Mullin, 2008; Zuriguel et al., 2008; Zuriguel et al., 2007). The free-field pressure cells developed by Askegaard (1989) were adopted in this study.

The relative size of the pile to the particle size may be an important factor for consideration. Relatively large scale pile tests produce rather consistent pressure measurements for same preparation procedure. Generally these tests support the concept that the pressure dip is a robust phenomenon for a pile formed by pouring particles with funnel feeding. The most commonly referenced experimental evidence is the early study ofSmid and Novosad (1981) who used quartz sand and granulated fertilizer NPK-1 and observed a significant pressure minimum at ~35% of the anticipated hydrostatic value γH_p (Fig. 2). By contrast with these relatively large scale pile tests, small scale tests often suffered from significant fluctuations in

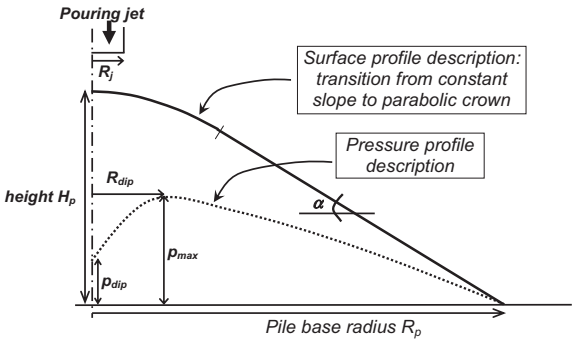

Fig. 2. Description of surface and pressure profiles of a sandpile with a central dip.

the deduced pressures. In such tests, it is often necessary to average many repeated experiments before a pressure dip can be seen (e.g. Brockbank et al., 1997; Geng et al., 2001; Zuriguel and Mullin, 2008; Zuriguel et al., 2008; Zuriguel et al., 2007). These results have led some to believe that the pressure dip is not a securely reproducible phenomenon and that its formation can be sensitive to numerous factors. In this study,relatively large conical pile laboratory experiments were conducted in which the base pressure distribution was measured with good accuracy.

The size of the pressure dip has been found to depend on the pile shape. Conical piles often have a pronounced pressure dip. The dip pressure p_{dip} relative to the "null-hypothesis" hydrostatic pressure beneath the pile apex γH_p, has been widely found to be small (~35% by Smid and Novosad (1981); Vanel et al. (1999) and Ooi et al. (2008); 42–55% by McBride (2006)). By contrast, no dip or a negligible dip has been found in a wedge-shaped or prismatic pile (e.g. Lee and Herington, 1971; Trollope, 1956; Wiesner,2000). Vanel et al. (1999) observed a clear dip in their test on a prismatic sand pile, but the dip was still significantly less than that in the conical pile. Sometimes the magnitude of pressure fluctuations is comparable with the magnitude of the dip being measured (e.g. Lee and Herington, 1971). However, for a pseudo-two dimensional pile – consisting of a single layer of particles, a substantial dip can still be observed. For example, by

averaging the results from a large number of repeated notionally identical tests (up to 500 tests), a normalised dip pressure up to 50% was measured in piles of photoelastic disks (Geng et al., 2001; Zuriguel and Mullin, 2008; Zuriguel et al., 2007).

The deposition jet dimension has been shown to significantly affect the basepressure distribution. In particular, deposition through a narrow funnel gave a pronounced dip for a conical pile but the raining procedure, with grains deposited over the whole pile base, produced no dip (Geng et al., 2001; Vanel et al., 1999). However, no data is available for situations that lie between these two extremes. One of the objectives of this study is to fill this gap.

It has been reported that the dip is slightly smaller if the feeding jet is kept close to the pile apex so that the energy of impact of the particles remains constant (Vanel et al., 1999). The effect of pouring height was reported to be more significant in a 2D single layer pile test (Geng et al., 2001), where a fixed height point deposition produced a pronounced dip while a slowly moving point depositionproduced no pressure dip. The dependence of the pressure profile on the pouring height suggests that the impact energy of the particles may play a significant role in the formation of the pressure dip. The pouring rate may also have some effect, but no systematic studies of this are known.

There is also evidence that the dip depends on the properties of the particles such as their shape, stiffness, size and size distribution and surface roughness (Brockbank et al., 1997; Jotaki and Moriyama, 1979; Zuriguel and Mullin, 2008; Zuriguel et al., 2007). No thorough investigation of these aspects is known.

The overall experimental plan in the present study used a series of relatively large laboratory pile tests to investigate several factors that affect the base pressure profile. These include base deflection, the deposition process (pouring rate, pouring heightand pouring jet dimension), particle shape and particle size. All these factors have been speculated by others to influence the pressure dip, as outlined above. In this paper, only the tests that investigated the influence of different deposition processes are reported. Some preliminary results of the tests that used a concentrated pouring jet with and without base deflection were previously reported by Ooi et al. (2008).

2. Experiment

2.1. Test setup

The conical granular pile tests were conducted in a 3-floor experimental gantry which consists of the filling compartment, pile test compartment and reclaiming compartment as shown in Fig. 3.

As deflection of the base beneath the pile was previously shown to be a significant factor in producing a pressure dip (Ooi et al., 2008; Savage, 1998; Wiesner, 2000), the base was constructed to be rigid so that its effect was minimised. The base beneath the pile was constructed using a 9.5 mm thick circular aluminium plate placed on a 20 mm thick circular wooden plate which

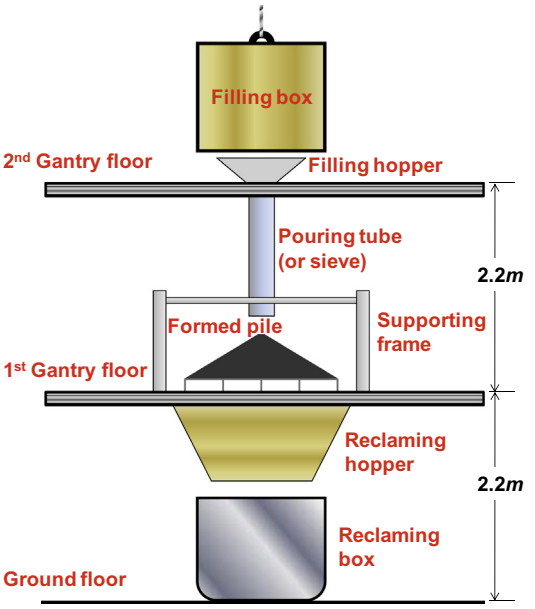

Fig. 3. Sketch of test setup in the experimental gantry with three levels used respectively for solid filling, pile test and solid reclaiming.

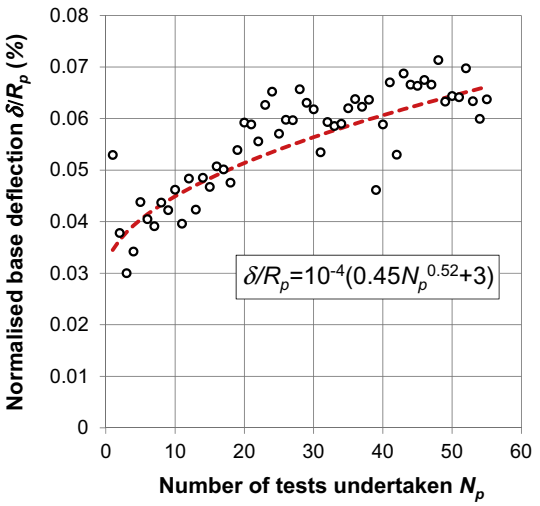

Fig. 4. Evolution of maximum base deflection. The dash-line is a power-law fit of the test data which shows a trend of gradual increase of the base deflection with number of tests conducted.

itself was supported on stiff steel girders. A layer of cement mortar 10–20 mm thick was placed between the wooden plate and the steel girders to ensure an even support. The base was made circular to allow the particles to flow over the edge, so the final pile radius was always exactly the same as the base radius ($R_p = R_b = 625$ mm) in all tests. This guaranteed a reliable repeatability of the tests.

During the tests, the central base deflection was monitored using an LVDT. The central deflection always remained rather small (well below 0.1% of the pile radius and 0.2% of the pile height). However, it was found that the central base deflection gradually increased as more

tests were conducted, which suggests that there was a slight degradation of the base due to usage (Fig. 4). According to Vanel et al. (1999), the influence of the base deflection should be negligible if the base deflection is less than 1% of the pile height.

2.2. Test granular solid

Small andapproximately spherical mini iron ore pellets (Fig. 5) were used to conduct the pile tests. The pellets had a very rough surface and were relatively uniform in size with a mean diameter of $d_p = 3.0$ mm and a size range of $2.36 < d_p < 4.00$ mm for 4.4–99.5% passing in a particle size analysis by dry sieving (Fig. 5). These particles are interesting because they are approximately spherical but sufficiently non-spherical to destroy the degenerate symmetry observed in spherical assemblies. This choice allows a comparison to be made with a recent 2D study involving elongated particles (Zuriguel et al., 2007), which are thought to produce a significantly larger pressure dip than circular particles. The pellets also had the added advantage that they have a high density, allowing a greater sensitivity in pressure measurement The loosest and densest bulk densities achieved in control tests using a cylindrical chamber were 2250 and 2400 kg/m^3, respectively.

Using a direct shear tester, the internal angle of friction for the pellets was measured to be 38.7° for loose packing and 44.1° for compact packing (Fig. 6). The loose packing here refers to the state of a sample prepared by slowly depositing pellets into the shear tester without any further disturbance before shear test. By contrast, the compact packing state was achieved by shaking and tapping the filled tester after particle placement. The internalfriction angle in the formed pile may well be smaller than the loose value (38.7°), since the confinement of the particles is less in the pile than in a chamber.

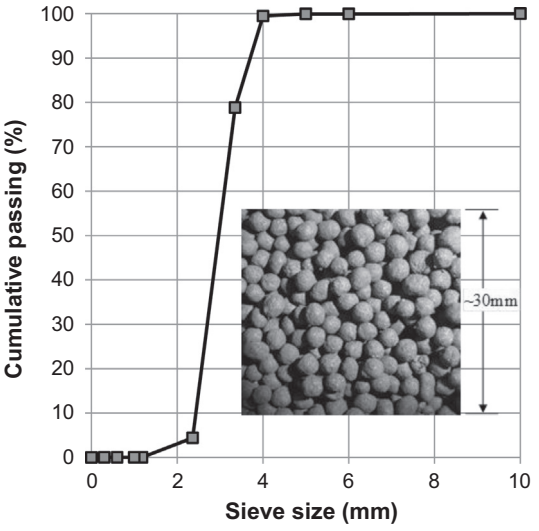

Fig. 5. Size distribution of mini iron pellets with mean diameter of $d_p = 3.0$ mm and size range of $2.36 < d_p < 4.00$ mm for 4.4–99.5% passing in a particle size analysis by dry sieving. The inset is a photo of the pellets.

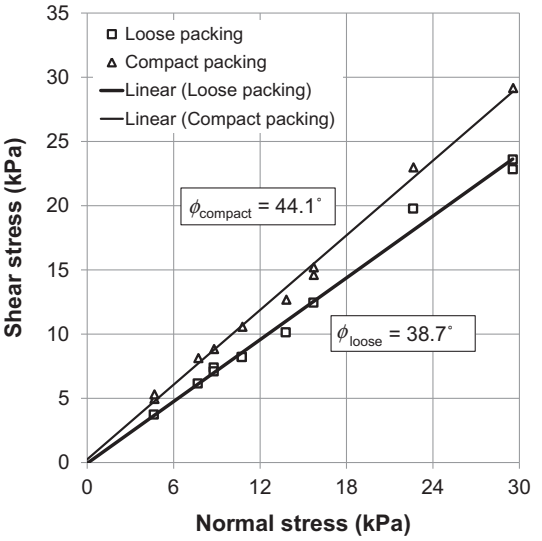

Fig. 6. Internal friction angle of test pellets determined using a direct shear tester. The linear regression best fits for loose sample (□) and compact sample (△) give friction angle of $\phi_{loose} = 38.7°$ and $\phi_{compact} = 44.1°$ respectively.

2.3. Pressure measurement

Free-field pressure cells have been widely used to observe pressures in granular media (Askegaard, 1978, 1981, 1986; Askegaard et al., 1971; Munch-Andersen, 1982). This study adopted the Askegaard pressure cell (Fig. 7) which was designed and manufactured by Askegaard (1989) using well documented and carefully tested procedures.

The cells have a diameter of 75 mm, which is 25 times larger than the mean particlesize, giving more than 400 contacts on each cell face. This makes the pressure measurement much less dependent on individual force chains in the solid, when compared with many smaller scale pile tests (e.g. Brockbank et al., 1997). Each pressure cell consists of a thin flat cylindrical chamber made of titanium filled with oil whose pressure is measured. The inner thickness of the chamber is approximately 0.1 mm and the total thickness of the cell, including the pressure transducer is 14 mm. A very high cell stiffness is guaranteed by the high incompressibility of oil, which ensures that the maximum face flexibility is below 10^{-2} μm/kPa. Each cell was calibrated with the cell embedded in a stiff granular solid in a specially designed calibration chamber to find its individual calibration coefficient.

Careful cell placement tests (e.g.Askegaard and Brown, 1995; Garnier et al., 1999) have confirmed that reliable and consistent pressure measurements in a granular medium can be achieved if appropriate precautions are taken in the cell placement, despite a small sensitivity of the measurements to the operator (i.e. personal factor). It may be noted the same type of cell was used by Evesque et al. (1999) when measuring the base pressure beneath a sand pile whose radius was about half that of pile studied here.

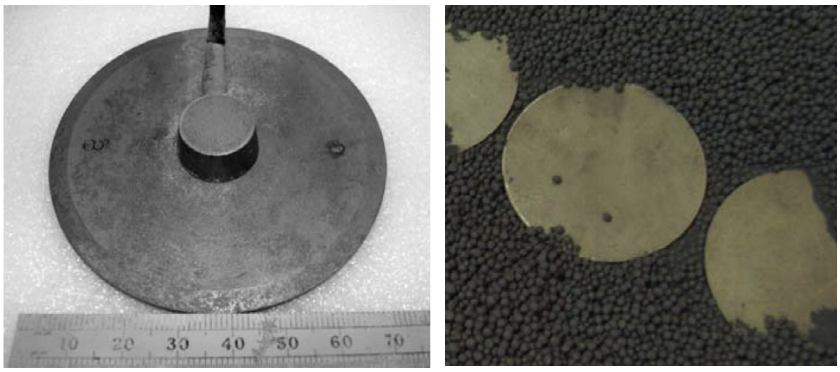

Fig. 7. Askegaard free-field pressure cell: (a) The cell face with pressure transducer; (b) when cells are partially embedded in pellets with flat face exposed upwards.

Table 1
Summary of pile tests.

Pile configuration ([a])		Deposition radius R_j/R_p	Deposition rate ([b]) q_{dep}/q_{dep}^{CSL}	Deposition height H_{dep}/R_p
Concentrated deposition	C–S–L	0.024	1	0.85
	C–I–L	0.04	4.6	0.85
	C–F–L	0.0448	6.4	0.85
	C–S–H	0.024	1	2.3
	C–I–H	0.04	4.6	2.3
Diffuse deposition	D–N	0.21	3.4	0.98
	D–W	0.37	~20	0.98

[a] : Deposition method: C – concentrated deposition, D – diffuse deposition; deposition rates: S – slow, I – intermediate, F – fast; deposition height: L – low, H – high; deposition radius: N – narrow, W – wide.
[b] : Deposition rate of configuration of C–S–L, q_{dep}^{CSL} = 0.41 kg/s.

In the present experiments, the pressure cells were first placed carefully at fixed positions on the flat aluminium base plate. A layer of pellets approximately 25 mm thick was then spread evenly so that the pressure cells were firmly embedded, with a thin layer covering each cell face. A Perspex sheet ring whose diameter was slightly larger than the basediameter, was installed around the base to retain this pre-laid layer of pellets surrounding the pressure cells. The top surface of this layer was taken as the nominal base of the pile and the pressure cell readings were taken as zero at this point. The changes in pressure were then recorded during the pile formation. The readings of the pressure cells were also calibrated by formally equating the integral of the pressure measurements that produced the total base reaction force to the total weight of the pellets deposited. Such an in situ calibration process can help to avoid any error arising from possible sensitivity of the measurements to different test materials, packing structures and stress levels.

2.4. Summary of tests

The test piles were next constructed either as concentrated deposition using narrow jets or as diffuse deposition using sieves at afixed height above the base. For concentrated deposition, three different rates of deposition via slightly varied jet aperture were used, together with two different pouring heights. For diffuse deposition, two different diameters of sieve were used. The conditions for each test were simply identified using three characters, such as C–S–L, to indicate the deposition method, rate of pour and pouring height. The deposition methods were concentrated C or diffuse D; the pouring rates were fast F, intermediate I or slow S; and the pouring heights were high H or low L. For the diffuse tests, the jet was either narrow N or wide W. The tests and their deposition parameters are summarised in Table 1.

The symbols used in this paper for the various parameters describing the pile geometry and the base pressure profile are indicated in Fig.2.

3. Results and discussions

3.1. Configuration C–S–L

A total of 12 notionally identical tests of the pile configuration case C–S–L (concentrated deposition with slow pouring rate and low pouring height) were completed. An example pile at the final stage is shown in Fig. 8 with its final surface profile in Fig. 9. The measurement

Fig. 8. A test pile of configuration C–S–L at the final stage of its formation. The final radius achieved was constant at R_p = 0.625 m for all piles by allowing particle overflow on the circular base.

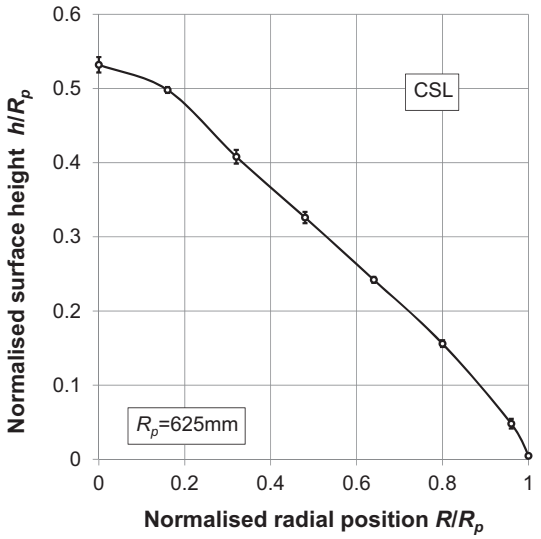

Fig. 9. Surface profile of pile configuration C–S–L. The error bars represent one standard deviation for 4 tests. The error of measurement is estimated at ±5 mm.

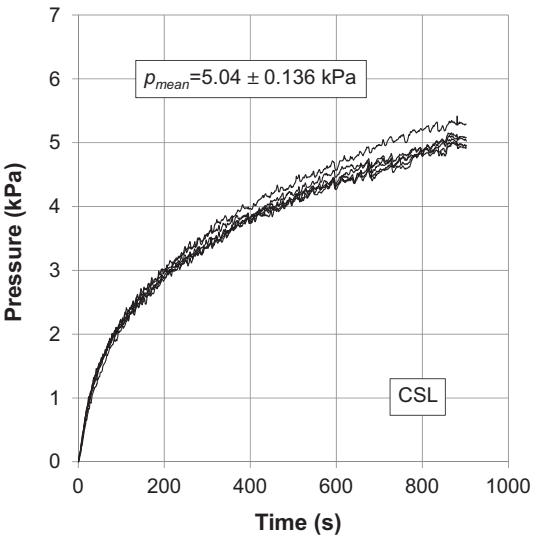

Fig. 10. Base pressure measured at different circumferential positions and a constant radius in a C–S–L test. The mean value of the measurements at the final stage is 5.04 kPa with a standard deviation of 0.14 kPa.

technique for the surface profile was made using a ruler and human reading, so some reading errors naturally existed which were estimated to be less than 5 mm. The rough character of the natural surface makes this shapeimperfectly quantifiable. The mean value of the angle of repose was determined from the middle of the conical slope, away from both the apex and the toe of the slope, and assessed as $\alpha = 28.0°$.

The pile volume was found by integrating the volume below the surface profile and was estimated to be close to $V = 0.165\ m^3$. The mass of the pile was measured to be $M = 341.5$ kg by direct weighing of the pellets. An estimate derived from the pouring rate and the pouring time indicated 345.8 kg, which showed that the pouring rate was accurately known. The bulk density deduced from the volume and mass was therefore $\rho_b = 2083\ kg/m^3$, which is smaller than the value found in the cylindrical container for the loose state ($2250\ kg/m^3$). It should be noted that the difficulties in accurately measuring the pile surface profile may have led to a slight overestimate of the pile volume, resulting in an underestimate of bulk density. If the surface was deemed to be everywhere 5 mm below the reported measurements, the deduced bulk density would be $2164\ kg/m^3$.

To determine whether the pressure distribution beneath a conical pile that has been centrally poured is axisymmetric, in one test pressure cells were placed around the circumference at a constant radius. Fig. 10 shows the evolution of pressure recorded by these six cells. They are very close to each other (maximum difference is <5%), showingthat no significant loss of symmetry is detectable. This justifies the assumption that the base pressure distribution may be obtained as a single valued function of radial coordinate, and that pressure cells could be placed at different circumferential locations to obtain a precise radial distribution with confidence.

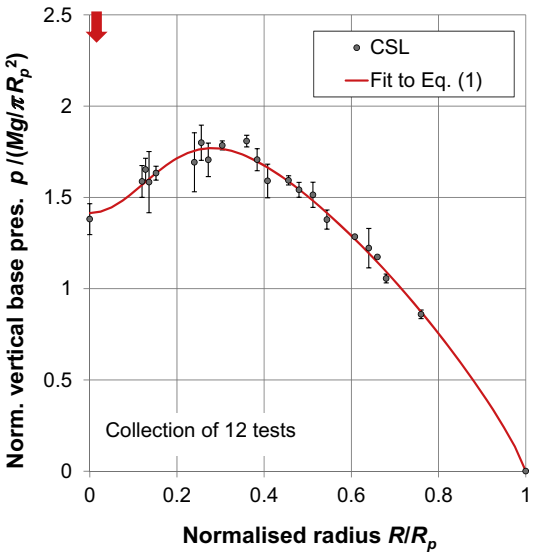

Fig. 11. Measured base pressure distribution in the C–S–L tests. The error bars are one standard deviation for 12 notionally identical tests. The solid line is a regression best fit of Eq. (1) with the fitted coefficients given in Table 2.

Fig. 11 shows the mean and scatter of the measured base pressure distribution at the end of the 12 tests of configuration C–S–L. The base pressure was normalised by the average base pressure $Mg/(\pi R_p^2)$ where M is the total mass and Rp is the outer radius of the pile. It shows a significant dipbeneath the apex, with the pressure rising steadily from the centre to a peak at a radius of $R \approx 0.3R_p$, before falling again towards the edge of the pile. The pressure profile is very similar in form to that in a smaller conical pile tested by Vanel et al. (1999) and that in a much larger gravel pile tested by McBride (2006). The results support the commonly stated proposition that an arching effect of some kind arises from the pile formation process which causes a significant part of the weight of solid in the central zone to be supported by an annular zone at larger radii. These results confirm and quantify the central local minimum in the base pressure distribution under a conical pile. It is shown to be a robust phenomenon that occurs naturally when the pile has been constructedusing a concentrated pouring jet.

The measured base pressure distribution $p(r)$ in Fig. 11 may be closely approximated by the following equation using five fitted coefficients a, b, n, r_1 and r_2:

$$p(r)/\frac{Mg}{\pi R_p^2} = a\left[\cos\left(\frac{\pi}{2}r\right)\right]^n - b\exp\left(-\left(\frac{r-r_1}{r_2}\right)^2\right) \qquad (1)$$

where r is the normalised radial coordinate (R/Rp). The right-hand side of the equation contains two parts. The first part represents the overall pressure profile. The second part represents the reduction of pressure associated with the pressure dip and centred at the normalised location r_1. The fitted coefficients for the mean of all tests using the configuration C–S–L are listed in Table 2. Equation (1) clearly fits the test data very well (Fig. 11).

Table 2
Fitted coefficients of Eq. (1) for test cases.

Cases	a	n	b	r_1	r_2
C–S–L	2.01	0.835	0.60	0	0.198
C–I–L	1.94	0.796	0.80	0	0.109
C–F–L	1.95	0.804	0.89	0.010	0.110
C–S–H	2.16	0.937	0.73	0	0.217
C–I–H	1.91	0.87	0.87	0	0.112
D–N	2.12	0.950	0.66	0.162	0.113
D–W	2.20	1.00	0.68	0.234	0.206
D–F	1.83	0.650	0.15	0.950	0.141

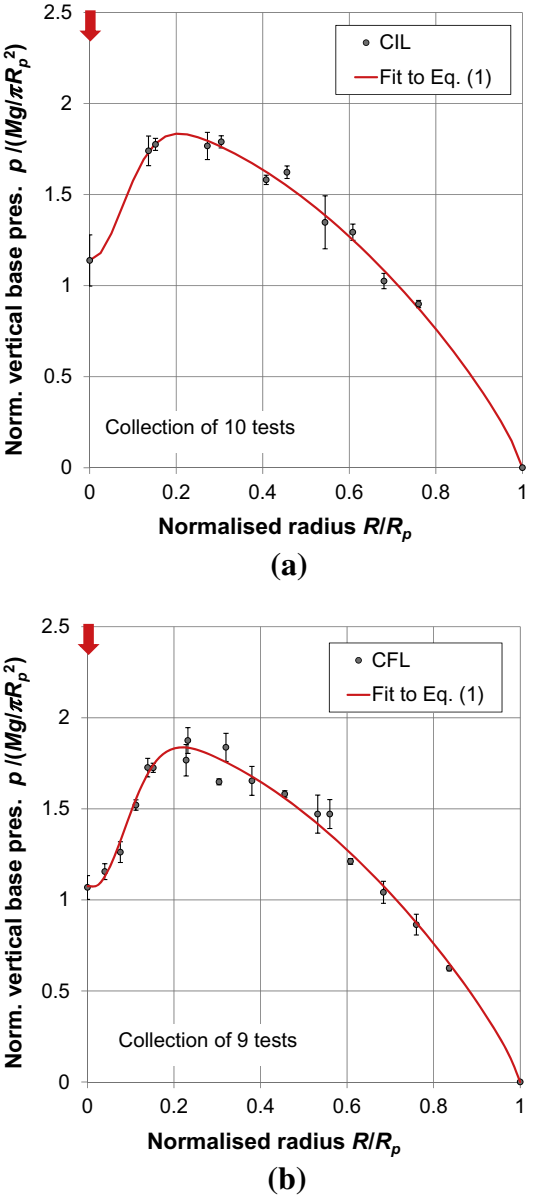

Fig. 12. Measured base pressure distribution in (a) C–I–L tests; and (b) C–F–L tests. The error bars in (a) (and (b)) are one standard deviations for 10 (and 9) notionally identical tests. The solid lines are regression best fits of Eq. (1) with the fitted coefficients given in Table 2.

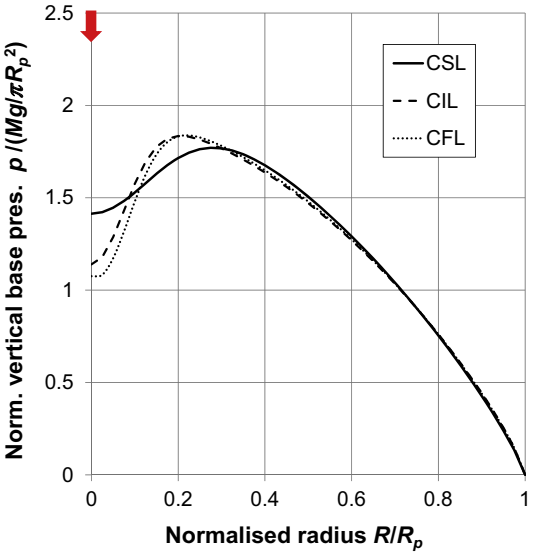

Fig. 13. Effect of deposition rate on the base pressure distribution shown with the best fit lines from Figs. 11, 12a and 12b.

The magnitude of the normalised dip pressure was determined using Eq. (1) and found to be $\bar{p}_{dip} = a - b = 1.41$.

3.2. Effect of pouring rate

The effect of pouring rate on the dip profile was studied by changing the size of the deposition aperture. The configurations C–I–L and C–F–L give respectively a 4.6 and 6.5 times increase in the pouring rate of configuration C–S–L. The measured base pressure profiles for these two increased pouring rates are shown in Fig. 12a and b. The pouring rate is seen to affect the pressure dip significantly. The normalised dip pressure $\bar{p}_{dip}$ reduced further from 1.41 in the slow pouring C–S–L tests to ~1.14 in the intermediate pouring C–I–L tests and to ~1.06 in the fast pouring C–F–L tests. Thus, although anincreased pouring rate can affect the pressure dip, this effect appears to be nonlinear, with significant changes in one region and much less effect in another. The three mean test results are shown in Fig. 13, where it is also evident that the width of the dip was reduced from about 0.3–0.2 with the increase of the pouring rate from 0.41 to 1.89 kg/s.

A key aspect of the pressure distribution beneath the pile is its progressive development. To explore the differences arising from different pouring rates in more detail, the evolution of the base pressure profile recorded during the construction is shown in Fig. 14a for one C–S–L test and in Fig. 14b for one C–I–L test.

For both piles,until 5 s after deposition began there is little evidence of any pressure dip. This is because the jet size is quite large compared with the pile size, so the impacting particles have a strong effect. Moreover, the diameter of each pressure cell is large compared with the size of the pile. As the pile grew bigger, the pressures in the outer zone increased a little faster than the reference hydrostatic pressure value, whilst the pressure in the central zone increased at a slower pace, progressively leading

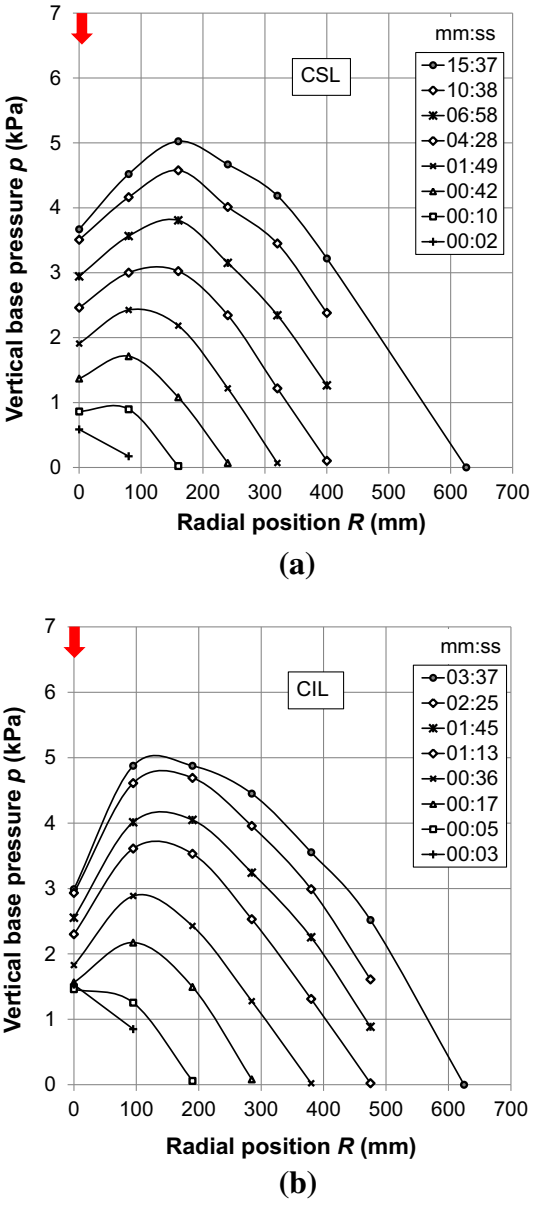

Fig. 14. Base pressure evolution for concentrated deposition: (a) a typical C–S–L test; (b) a typical C–I–L test.

towards a pressure dip that became steadily more pronounced. A key difference between the two pouring configuration cases is that each C–I–L test produced a more pronounced dip and did so faster than each C–S–L test.

During the early stages of deposition, when the pile size was small, it was observed that the particles spread from the apex in a continuous and axisymmetrically uniform fashion over the whole pile surface. This type of pileformation has previously been observed in silos (Nielsen, 1998). However, as the pile size increased, the particles were shed from the pile apex down the slope in a non-uniform and less intense manner. When the pile size increased further, the pellets were shed in intermittent avalanches. These changes are thought to be controlled by the relationship

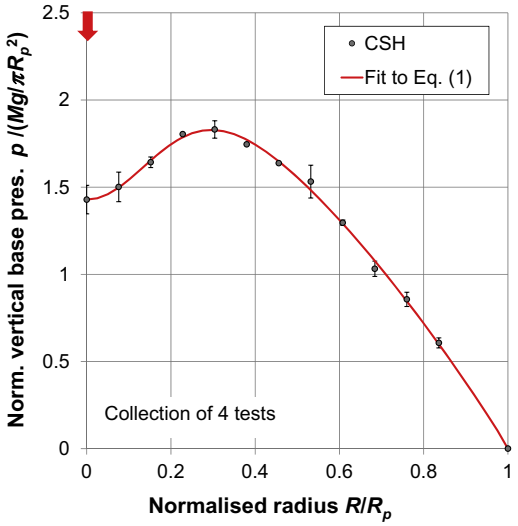

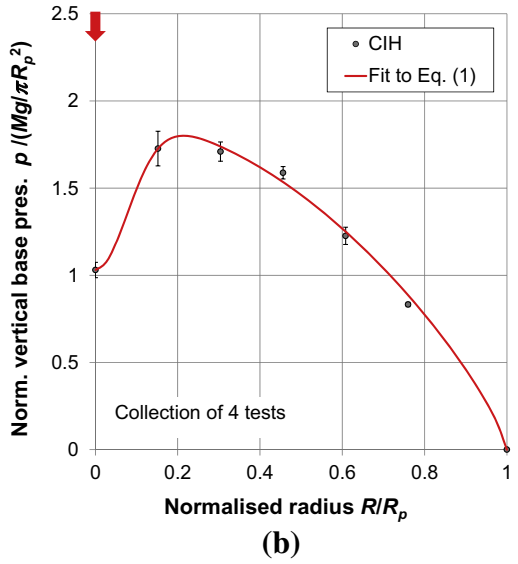

Fig. 15. Measured base pressure distribution for: (a) C–S–H tests; and (b) C–I–H tests. The error bars in (a) (and (b)) are one standard deviations for 4 (and 4) notionally identical tests. The solid lines are best fits of Eq. (1) with the fitted coefficients given in Table 2.

between the pile surface area, the jet size and the deposition rate. A low deposition rate is thought to be unable to sustain the uniform spreading seen at the outset. It is also suggested here that the pattern of particle repositioning within the total pile (e.g. by cascading from the apex down the slope) may play an important role in transferring stresses away from the centre towards the periphery. It seems probable that the flow rate and flow form (continuous or intermittent, uniform or non-uniform) of the cascading downslope flow are responsible for the differences between the sizeand width of the pressure dips seen in C–S–L and C–I–L.

Regardless of its magnitude, the progressive development of a pressure dip seen here supports the proposition that, for a macroscopic granular pile where the pile dimension is much larger than the dimension of the pouring jet, itself much larger than the mean particle size, a robust pressure profile with a central dip is a natural formation which occurs reproducibly. By contrast, some published results (e.g. Brockbank et al., 1997; Geng et al., 2001; Zuriguel et al., 2007) show considerable fluctuations and a much less well defined pressure dip even after a considerable amount of averaging over many repeated tests. It is probable that these fluctuations are caused by the relatively small ratio of pile to particle size in those experiments.

3.3. Effect of pouring height

A change of the pouring rate, from the same pouring height, produces a change in the impact power, so it is of interest to investigate the case where only the energy of impact is changed while the pouring rate is kept constant, thus separating the velocity of impact from the mass deposition rate. This was studied by conducting the test with different pouring heights and same pouring rate. Measured base pressure profiles of C–S–H tests (concentrated deposition with slow pouring rate and high pouring height) are shown in Fig. 15a. The profile changed little when the pouring height was increased to 2.7 times of that of the C–S–L tests (Fig. 16). The same observation may also be made for the C–I–L and C–I–H tests with a larger pouring rate shown inFig. 16. Therefore, based on these observations, the pressure distribution on the pile base is not significantly affected by the pouring height, within the tested parameter ranges. This observation is at variance with the early study of Geng et al. (2001), where a fixed pouring height produced a large pressure dip, but a slow deposition with minimised pouring height produced no dip. Nevertheless, it is possible that the effect of pouring height only

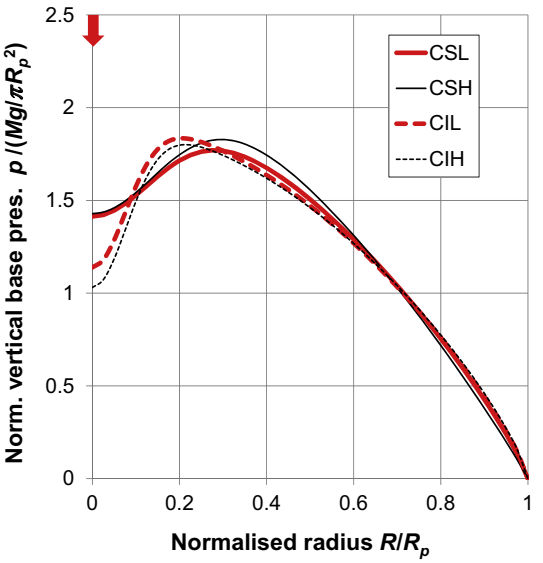

Fig. 16. Effect of deposition rate on the base pressure distribution shown with best fit lines from Figs. 11, 12a, 15a and b.

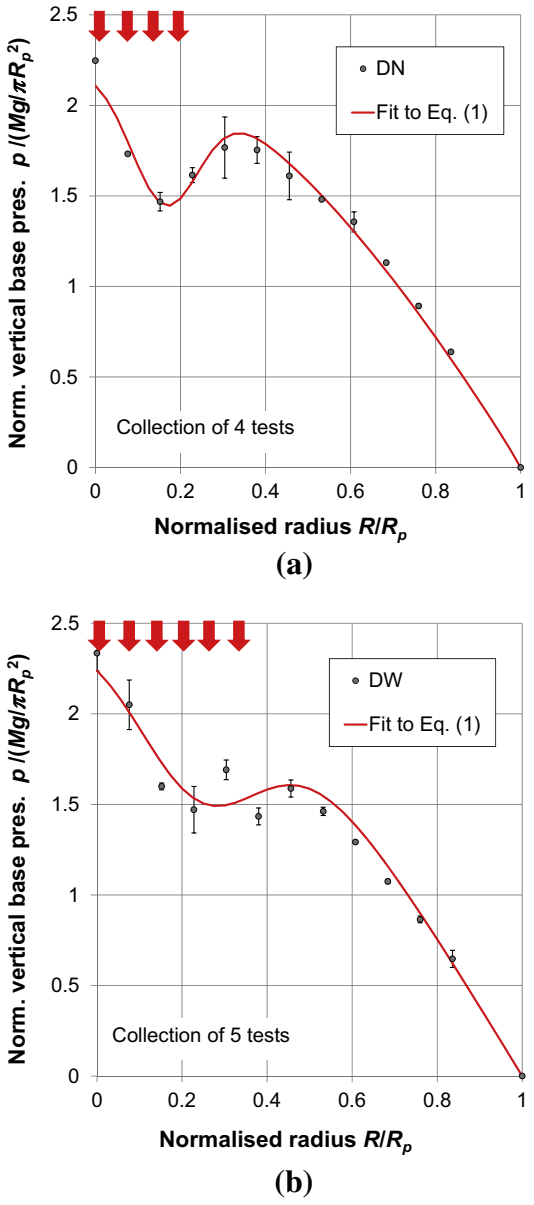

Fig. 17. Measured base pressure distribution for: (a) D–N tests and (b) D–W tests. The error bars in (a) (and (b)) are one standard deviations for 4 (and 5) notionally identical tests. The solid lines are best fits of Eq. (1) with the fitted coefficients given in Table 2.

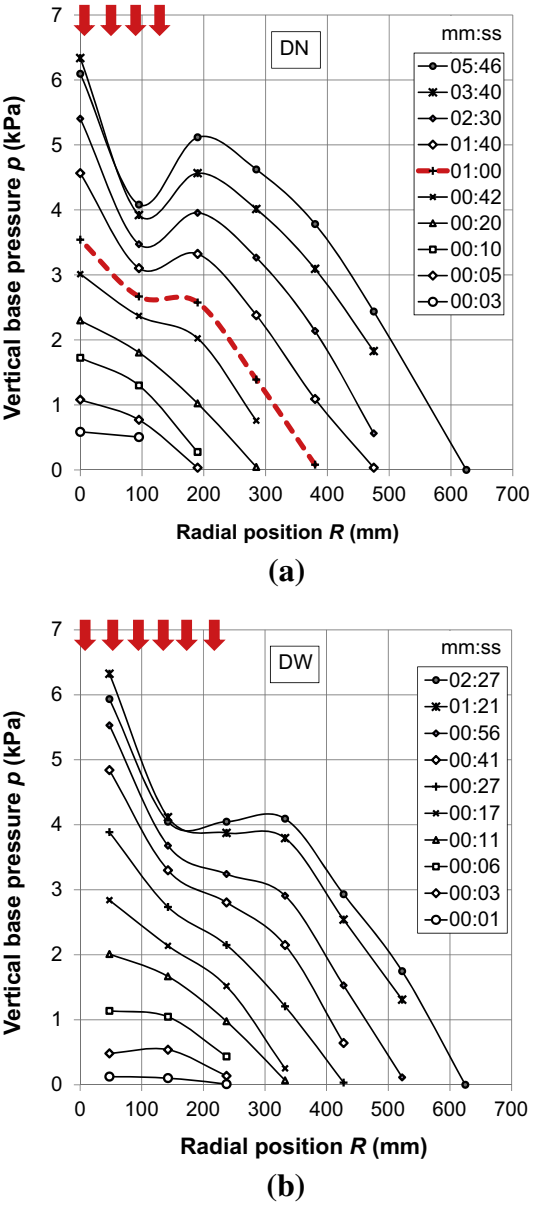

Fig. 18. Base pressure evolution for diffuse deposition: (a) a typical D–N test; (b) a typical D–W test.

becomes significant when it is relatively small, and that the critical height for such effects to be observed lies below the pouring height studied here ($H_{dep} = 0.85H_p$).

3.4. Effect of deposition or jetradius

The effect of the radius of deposition (jet radius) may be of greater importance in understanding the underlying mechanism of the pressure dip phenomenon. Apart from the narrow jet deposition described above, this study also investigated more diffuse deposition cases with two different jet radii: $R_j/R_p = 0.21$ (configuration D–N) and $R_j/R_p = 0.37$ (configuration D–W). The measured base pressure profiles are shown in Fig. 17a and b respectively. A striking feature of the observations is that the pressure dip is not only reduced as the jet radius is increased, but the location of the dip is shifted away from the centre towards theedge of the deposition jet. A pressure hump developed in the centre in contrast to a pressure dip that commonly developed under concentrated deposition.

These patterns suggest that the pressure dip develops at the radial position where cascading downslope flows begin during pile formation, rather than simply at the pile centre. In the region near the pile centre and away from the slope, particles tend to be placed in horizontal layers (mainly

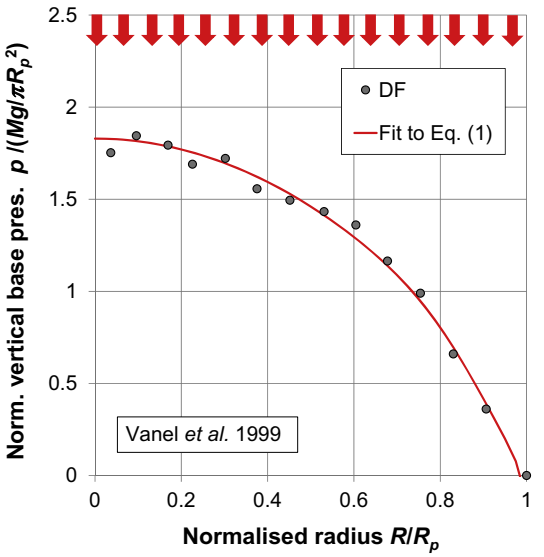

Fig. 19. Base pressure in full diffuse deposition (D–F) tests. Each data point represents an average of 10–12 independent tests. (Redrawn after Vanel et al. (1999)).

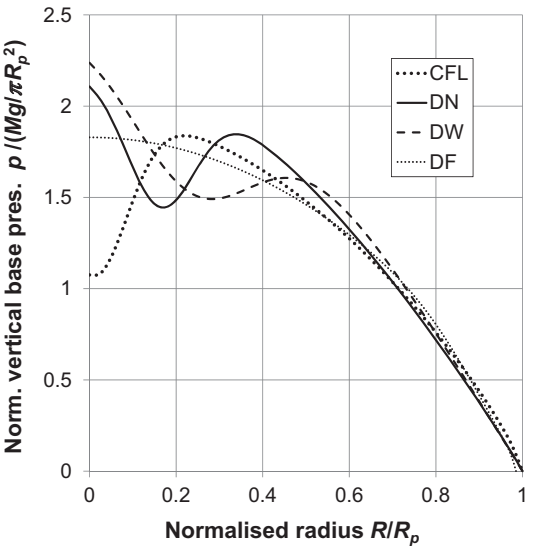

Fig. 20. Effect of deposition radius on base pressure distribution shown with the best fit lines from Figs. 12b, 17a, 17b and 19.

remaining close to their original position), instead of forming inclined layers as a result of downslope flows. These contrasting patterns of deposition were also observed during silo filling by Nielsen (1998), but were attributed to the effects of particle shape.

The development of the displaced dip is best examined by showing its progressive evolution. The progressive development of the base pressure profile in a D–N and a D–W test areshown in Fig. 18a and b respectively. In the early stage when the pile radius was less than twice the deposition radius, the maximum base pressure appeared right at the centre, with no pressure dip. This is consistent with the observation of Vanel et al. (1999) that no pressure dip occurred when the pouring jet was as wide as the base radius (i.e. fully diffuse (Fig. 19)). As the pile size increased, the pressure at both the centre and the outer zone increased faster and overtook the pressure in the intermediate zone where a dip was eventually formed.

As the deposition radius in the D–W tests was larger than that in the D–N tests, there is a time during the D–N test when the relative deposition radius is comparable to that in the D–Wtest at the final stage. This instant lies between deposition times 01:00 and 01:40 mm:ss from the start of the test. The pressure profile at 01:00 mm:ss in the D–N test is denoted by a dotted line in Fig. 18a. Clearly the shape of the denoted profile is very similar to that of the final profile in the D–W test (Fig. 18b).

These observations give further support to the proposition that the dip forms at, or adjacent to, the radial position at which cascading downslope flows first occur. For a pile with a given jet radius, the central pressure increases in a fashion similar to that in a pile formed by fully-raining deposition. The pressure dip then forms at a radius slightly inside the edge of the deposition jet where downslope flows start to occur. At later stages of pile formation, surface flows come to dominate andthe pressure increases much faster in the outer zone than in other locations and eventually overtakes the central pressure. When the pile radius is significantly larger than the deposition jet radius, the pressure pattern evolves into a narrow jet deposition configuration where the central peak completely disappears.

The pressure profiles in the diffuse deposition tests can also be fitted by Eq. (1) as shown in Figs. 17 and 19. The best fit coefficients for these tests are listed in Table 2. The effect of deposition radius on the base pressure profile is summarised in Fig. 20, where an evolution of the pressure dip size and location is clearly illustrated.

4. Conclusions

A systematic experimental investigation of the pressure dip phenomenon in a conical pile under different deposition conditions including pouring rate, pouring height and deposition jet dimension has been presented in this paper. The results have shown that the base pressure distribution, at the macroscopic scale, has a central dip beneath the apex of the pile that is a repeatable and robust phenomenon for a concentrated deposition. An increase of the pouring rate may enhance the magnitude of the dip and reduce its width, but an increase in the pouring height has a negligible effect within the studied range. When the deposition jet radius is significantly smaller than the final pile radius, the dip that develops at the centre of the base is the same as that shown in previous studies. However, when the deposition radius is large relative to the final pile radius, the locationof the dip is moved towards the edge of the deposition jet, with some recovery in the central pressure peak. It is proposed that the particle flows down the conical slope of the pile during its formation may be an important contributor for the formation of the pressure dip. The pressure dip may be closely related to the starting location, intensity and form of the downslope flows.

Acknowledgements

We acknowledge the support from the EPSRC (Grant GR/T23541) and the Scottish Funding Council for the Joint Research Institute with the Heriot-Watt University which is a part of the Edinburgh Research Partnership in Engineering and Mathematics (ERPem). J.A. also acknowledges the support from an Edinburgh University Research Scholarship and further support from the EPSRC (Grant EP/H011951/1) for his work at Nottingham University after completing his PhD. The miniiron ore pellets were provided by LKAB Group, Sweden. The authors are grateful to Dr I. Zuriguel, Prof. T. Mullin, Prof. R.P. Behringer and Dr J. Geng for many helpful discussions on this topic, to C. Brown for the discussions on pressure cell measurements, and to Chris A. Millar, Edward C.P. Nash, Brendan S. Bradley and David G. Holmes for their assistance in conducting the experimental tests.

References

Ai, J., Chen, J.-F., Ooi, J.Y., 2013. Finite element simulation of the pressure dip in sandpiles. Int. J. Solids Struct. 50, 981–995. http://dx.doi.org/10.1016/j.ijsolstr.2012.12.006.

Ai, J., Chen, J.F., Rotter, J.M., Ooi, J.Y., 2011. Numerical and experimental studies of the base pressures beneath stockpiles. Granular Matter 13, 133–141. http://dx.doi.org/10.1007/s10035-010-0215-6.

Askegaard, V., 1978. Stress and strain measurements in solid materials, Report No.92. Structural research laboratory, Technical University of Denmark, Lyngby.

Askegaard, V., 1981. Design and application of stress and strain cells with small measuring errors. NDT Int. 14, 271–277.

Askegaard, V., 1986. Consequence of loading history on the measuring error of embedded stress cells. In: Proceedings of the Second International Conference on Bulk Materials Handling and Transportation, Institution of Engineers, Wollongong, Australia, pp. 138–142.

Askegaard, V., 1989. Three component pressure cells for steel model silo, Report S.8817. Department of Structural Engineering, Technical University of Denmark.

Askegaard, V., Bergholdt, M., Nielsen, J., 1971. Problems in connection with pressure cell measurements in silos. Bygningsstatiske Meddeselser 42, 33–74.

Askegaard, V., Brown, C., 1995. Influence of personal factor on cell response when mounting embedded pressure cells. Bulk Solids Handling 15, 221–224.

Atman, A.P.F., Brunet, P., Geng, J., Reydellet, G., Claudin, P., Behringer, R.P., Clément, E., 2005. From the stress response function (back) to the sand pile 'dip'. Eur. Phys. J.E 17, 93–100. http://dx.doi.org/10.1140/epje/i2005-10002-2.

Brockbank, R., Huntley, J.M., Ball, R.C., 1997. Contact force distribution beneath a three-dimensional granular pile. J. Phys. I 7, 1521–1532. http://dx.doi.org/10.1051/jp2:1997200.

Cates, M.E., Wittmer, J.P., Bouchaud, J.P., Claudin, P., 1998. Development of stresses in cohesionless poured sand. Philos. Trans. R. Soc. A 1998, 2535–2560. http://dx.doi.org/10.1098/rsta.1998.0285.

Didwania, A., Cantelaube, F., Goddard, J., 2000. Static multiplicity of stress states in granular heaps. P. R. Soc. Lond. A Mater. 456, 2569–2588. http://dx.doi.org/10.1098/rspa.2000.0626.

Evesque, P., Noblet, S., Rault, G., 1999. Stress in conic piles determined by a centrifuge experiment: breakdown of scaling hypothesis. Phys. Rev. E 59, 6259–6262. http://dx.doi.org/10.1103/PhysRevE.59.R6259.

Garnier, J., Ternet, O., Cottineau, L., Brown, C., 1999. Placement of embedded pressure cells. Geotechnique 49, 405–414. http://dx.doi.org/10.1680/geot.1999.49.3.415.

Geng, J., Longhi, E., Behringer, R.P., Howell, D.W., 2001. Memory in two-dimensional heap experiments. Phys. Rev. E 64, 060301. http://dx.doi.org/10.1103/PhysRevE.64.060301.

Hummel, F.H., Finnan, E.J., 1921. The distribution of pressure on surfaces supporting a mass of granular material. Proc. Inst. Civil Eng. 212, 369–392. http://dx.doi.org/10.1680/imotp.1921.14900.

Jotaki, T., Moriyama, R., 1979. On the bottom pressure distribution of the bulk materials piled with the angle of repose. J. Soc. Powder Technol. Jpn. 16, 184–191.

Lee, I.K., Herington, J.R., 1971. Stresses beneath granular embankments. In: Proceedings of the 1st Australia–New Zealand Conference on Geomechanics 1, Melbourne, pp. 291–296.

Liffman, K., Chan, D.Y.C., Hughes, B.D., 1992. Force distribution in a two dimensional sandpile. Powder Technol. 72, 255–267 (doi:dx.doi.org/10.1016/0032-5910(92)80044-W).

Liffman, K., Chan, D.Y.C., Hughes, B.D., 1994. On the stress depression under a sandpile. Powder Technol. 78, 263–271 (doi:dx.doi.org/10.1016/0032-5910(93)02801-G).

Liffman, K., Nguyen, M., Metcalfe, G., Cleary, P., 2001. Forces in piles of granular material: an analytic and 3D DEM study. Granular Matter 3, 165–176. http://dx.doi.org/10.1007/s100350100086.

McBride, W., 2006. Base pressure measurements under a scale model stockpile. Part. Sci. Technol. 24, 59–70. http://dx.doi.org/10.1080/02726350500403264.

Michalowski, R.L., Park, N., 2004. Admissible stress fields and arching in piles of sand. Geotechnique 54, 529–538. http://dx.doi.org/10.1680/geot.2004.54.8.529.

Munch-Andersen, J., 1982. Measuring of internal stresses in a granular media. In: Euromech 157: Quality of Mechanical Observations on Particulate Media, Copenhagen, pp. Y1–Y4.

Nedderman, R.M., 1992. Statics and Kinematics of Granular Materials. Cambridge University Press, Cambridge, UK.

Nielsen, J., 1998. Pressures from flowing granular solids in silos. Philos. Trans. R. Soc. A 356, 2667–2684. http://dx.doi.org/10.1098/rsta.1998.0292.

Ooi, J.Y., Ai, J., Zhong, Z., Chen, J.F., Rotter, J.M., 2008. Progressive pressure measurements beneath a granular pile with and without base deflection. In: Chen, J.F., Ooi, J.Y., Teng, J.G. (Eds.), Structures and Granular Solids: From Scientific Principles to Engineering Applications. CRC Press, London, pp. 87–92, DOI: 10.1201/9780203884447.ch8.

Savage, S.B., 1997. Problems in the statics and dynamics of granular materials. In: Behringer, R.P., Jenkins, J.T. (Eds.), Powders and Grains 97. Balkema, Rotterdam, Netherlands, pp. 185–194.

Savage, S.B., 1998. Modeling and granular material boundary value problems. In: Herrmann, H.J. (Ed.), Physics of Dry Granular Media. Kluwer Academic Publishers, pp. 25–96.

Smid, J., Novosad, J., 1981. Pressure distribution under heaped bulk solids. In: Proceedings of 1981 Powtech. Conf., Ind. Chem. Eng. Symp., p. 63.

Trollope, D.H., 1956. The Stability of Wedges of Granular Materials. University of Melbourne.

Vanel, L., Howell, D., Clark, D., Behringer, R.P., Clément, E., 1999. Memories in sand: experimental tests of construction history on stress distributions under sandpiles. Phys. Rev.E 60, R5040–R5043. http://dx.doi.org/10.1103/PhysRevE.60.R5040.

Wiesner, T.J., 2000. Failure stresses beneath granular embankments. In: Smith, D.W., Carter, J.P. (Eds.), Developments in Theoretical Geomechanics: The John Booker Memorial Symposium. Balkema, Rotterdam, pp. 33–41.

Wittmer, J.P., Cates, M.E., Claudin, P., 1997. Stress propagation and arching in static sandpiles. J. Phys. I 7, 39–80. http://dx.doi.org/10.1051/jp1:1997126.

Wittmer, J.P., Claudin, P., Cates, M.E., Bouchaud, J.P., 1996. An explanation for the central stress minimum in sand piles. Nature 382, 336–338. http://dx.doi.org/10.1038/382336a0.

Zuriguel, I., Mullin, T., 2008. The role of particle shape on the stress distribution in a sandpile. Proc. R. Soc. Lond. A Mater. 464, 99–116. http://dx.doi.org/10.1098/rspa.2007.1899.

Zuriguel, I., Mullin, T., Arévalo, R., 2008. Stress dip under a two-dimensional semipile of grains. Phys. Rev. E 77, 061307. http://dx.doi.org/10.1103/PhysRevE.77.061307.

Zuriguel, I., Mullin, T., Rotter, J.M., 2007. Effect of particle shape on the stress dip under a sandpile. Phys. Rev. Lett. 98, 028001. http://dx.doi.org/10.1103/PhysRevLett.98.028001.